

Journal of Mechanics of Materials and Structures

**THERMAL STRESS AROUND AN ELLIPTIC HOLE
WEAKENED BY ELECTRIC CURRENT IN AN
INFINITE THERMOELECTRIC PLATE**

Kun Song, Hao-Peng Song, Peter Schiavone and Cun-Fa Gao

Volume 14, No. 1

January 2019



THERMAL STRESS AROUND AN ELLIPTIC HOLE WEAKENED BY ELECTRIC CURRENT IN AN INFINITE THERMOELECTRIC PLATE

KUN SONG, HAO-PENG SONG, PETER SCHIAVONE AND CUN-FA GAO

We propose effective strategies to manage thermal stress around an elliptic hole induced by electric current and heat flux in a thermoelectric material. Our results indicate that the thermal stress can be reduced dramatically, with little influence on conversion efficiency, by simply adjusting the value of the electric current. In fact, we find that additional electric current in the vertical direction can totally neutralize the thermal stress at a particular point, including the thermal stress singularity at a crack tip.

1. Introduction

Thermoelectric materials have the ability to convert heat directly into electric power and vice versa. Such materials are particularly advantageous in that they are noiseless, have no mechanical moving parts, and create no pollution. The use of thermoelectric materials has been pervasive in many different applications [Zhao and Tan 2014; Riffat and Ma 2003; Tritt and Subramanian 2006] but their lower thermal-electric conversion efficiency precludes their use as alternatives to traditional engines.

Much effort has been devoted to the optimization of the performance of thermoelectric materials; for example, the incorporation of nanoinclusions [Kim et al. 2006; Pei et al. 2011] and the continual development of manufacturing processes [Okamura et al. 2010; Kim and Chun 2007] as well as to the optimization of thermoelectric devices [Xuan 2002; Gökten 36; Omer and Infield 1998]. A crucial part of this ongoing progress is the simultaneous development of mathematical models and theoretical analyses required to support and guide overall progress in this area. For example, Callen [1960] has proposed the governing equations of a thermoelectric medium; Liu [2012] has developed a continuum theory for thermoelectric bodies in the framework of continuum mechanics while adhering to the general principles of thermodynamics; effective thermoelectric behavior of layered heterogeneous media has been studied by Yang et al. [2012]; Song et al. [2017] have discussed the overall macroperformance of a multilayered thermoelectric medium. These studies have led to dramatic improvements in the performance of thermoelectric devices as well as rapid recent developments in both their design and application.

Reliability and lifespan are also important factors to be considered in thermoelectric devices since most thermoelectric materials have relatively inferior mechanical properties. It has been shown that even in the absence of mechanical restraints, temperature gradients in thermoelectric materials create complex mechanical stress distributions, which are particularly severe in high performance media and difficult to counteract via free deformation [Choi et al. 2011; Yu et al. 2012]. In contrast to classical materials, simply connected thermoelectric media also suffer from the induction of thermal stresses, leading to,

Keywords: thermoelectric material, thermal stress, electric current.

for example, a (thermal stress) singularity of order $r^{-1/2}$ at the tip of an impermeable crack [Song et al. 2015]. Research into the suppression of thermal stress in thermoelectric systems, however, remains relatively rare. This can be attributed to the complex nature of the mathematical models involved. It is this particular area of endeavor that motivates our present study.

In this paper, we utilize complex variable methods to analyze the thermal stress in the vicinity of an elliptic hole present in a thermoelectric plate. Our study allows us to propose different strategies for dealing with induced thermal stress in thermoelectric materials. Firstly, our numerical analyses show that a simple adjustment of electric current can dramatically suppress the thermal stress in a thermoelectric medium while having little influence on the conversion efficiency. Secondly, additional electric current in the vertical direction is shown to be effective in entirely neutralizing the thermal stress at a particular point; for example, the thermal stress singularity at a crack tip can be eliminated by the introduction of electric current in the vertical direction. Each of these findings are significant in that they provide relatively simple yet effective ways of dealing with thermal stress in thermoelectric devices.

2. Governing equations

2.1. Electric fields. Consider a two-dimensional thermoelectric material occupying a Cartesian plane described by a generic point (x, y) . The coupled transport of electric current and heat flux means that the temperature field and the electric potential in the material depend explicitly on position and are thus here denoted by $T(x, y)$ and $\phi(x, y)$, respectively. We assume further that all material parameters are temperature independent so that, in particular, the electric conductivity σ and Seebeck coefficient S for this thermoelectric material are taken to be uniform. The governing equation for the electric current density \mathbf{J} in the thermoelectric material can then be expressed as [Milton 2002]

$$-\mathbf{J} = \sigma \nabla \phi + \sigma S \nabla T. \quad (1)$$

Since the charge is restricted in a standalone system, the electric current is conserved. Consequently,

$$\nabla \cdot \mathbf{J} = 0. \quad (2)$$

Substituting (1) into (2), we have

$$\nabla^2(\phi + ST) = 0. \quad (3)$$

The general solution of (3) is written in terms of the analytic function $f(z)$ of the complex variable $z = x + iy$ as

$$\phi + ST = \operatorname{Re}[f(z)]. \quad (4)$$

Substituting (4) into (1), the components of the electric current density can be expressed as

$$J_x = -\frac{1}{2}\sigma(f'(z) + \overline{f'(z)}), \quad (5)$$

$$J_y = -\frac{1}{2}\sigma i(f'(z) - \overline{f'(z)}), \quad (6)$$

so that

$$J_x - iJ_y = -\sigma f'(z). \quad (7)$$

2.2. Thermal fields. In a thermoelectric material, the heat flux \mathbf{Q} is induced by the coupled electric current and negative local temperature gradient and is written as [Callen 1960]

$$\mathbf{Q} = TS\mathbf{J} - \kappa\nabla T, \quad (8)$$

where κ is the thermal conductivity. In contrast to heat conduction in traditional materials, the heat flux in a thermoelectric material is not conserved as a result of Joule heating. Both the electric power and heat flux constitute the total energy flux \mathbf{U} such that [Yang et al. 2012]

$$\mathbf{U} = \mathbf{Q} + \phi\mathbf{J} = (\phi + ST)\mathbf{J} - \kappa\nabla T. \quad (9)$$

We restrict our system to be conserved, such that the energy flux is divergence-free,

$$\nabla \cdot \mathbf{U} = 0. \quad (10)$$

Substituting (9) into (10), and noting (4), we have

$$\nabla^2 T + \frac{\sigma}{\kappa} f'(z) \overline{f'(z)} = 0, \quad (11)$$

where the overbar denotes the complex conjugate. Solving (11), the temperature field can be expressed in the form

$$T = -\frac{\sigma}{4\kappa} f(z) \overline{f(z)} + g(z) + \overline{g(z)} + N, \quad (12)$$

where $g(z)$ is an arbitrary analytic function and N is an arbitrary real constant which denotes the uniform temperature field. The electric potential can be derived by substituting (12) into (4) as

$$\phi = \frac{\sigma S}{4\kappa} f(z) \overline{f(z)} + \frac{1}{2}(f(z) + \overline{f(z)}) - S(g(z) + \overline{g(z)}) - SN. \quad (13)$$

Finally, the thermal flux and energy flux can be deduced from (8) and (9) as

$$Q_x - iQ_y = \sigma f'(z) \left[\frac{1}{2} \overline{f(z)} \left(\frac{\sigma S}{2\kappa} f(z) + 1 \right) - S(2 \operatorname{Re}[g(z)] + N) \right] - 2\kappa g'(z), \quad (14)$$

$$U_x - iU_y = -\frac{1}{2} \sigma f(z) f'(z) - 2\kappa g'(z). \quad (15)$$

Since the temperature/electric potential and electric current/heat/energy flux have been expressed in terms of the two analytic functions $f(z)$ and $g(z)$, the corresponding thermal-electric problems in a two-dimensional thermoelectric system will be solved completely if the two analytic functions f and g are identified.

2.3. Stress field. The corresponding Airy (thermal) stress function Φ should satisfy the following compatibility equation [Parkus 1968; Timoshenko and Goodier 1951]

$$\nabla^4 \Phi + E\alpha \nabla^2 T = 0, \quad (16)$$

where α is the thermal expansion coefficient and E is Young's modulus. The general solution of (16) consists of the general solution of the biharmonic equation denoted here by Φ_0 added to a particular solution Φ_p of (16):

$$\Phi = \Phi_0 + \Phi_p. \quad (17)$$

In fact [Muskhelishvili 1975],

$$\Phi_0 = \frac{1}{2}(\bar{z} \varphi(z) + z \overline{\varphi(z)} + \theta(z) + \overline{\theta(z)}), \quad (18)$$

where $\varphi(z)$ and $\theta(z)$ are two analytic functions. Noting (12), the particular solution of (16) can be chosen as

$$\Phi_p = \frac{E\alpha\sigma}{16\kappa} h(z) \overline{h(z)}, \quad (19)$$

where

$$h(z) = \int f(z) dz. \quad (20)$$

Thus, the solution Φ can be expressed as

$$\Phi = \frac{1}{2}(\bar{z} \varphi(z) + z \overline{\varphi(z)} + \theta(z) + \overline{\theta(z)}) + \frac{E\alpha\sigma}{16\kappa} h(z) \overline{h(z)}. \quad (21)$$

We introduce the complex function $\psi(z)$ as the derivative of $\theta(z)$ with respect to z , thus the stress components can be deduced from (21) as

$$\sigma_{11} + \sigma_{22} = 4 \frac{\partial^2 \Phi}{\partial z \partial \bar{z}} = 2(\varphi'(z) + \overline{\varphi'(z)}) + \frac{E\alpha\sigma}{4\kappa} f(z) \overline{f(z)}, \quad (22)$$

$$\sigma_{22} - \sigma_{11} + 2i\sigma_{12} = 4 \frac{\partial^2 \Phi}{\partial z^2} = 2(\bar{z} \varphi''(z) + \psi'(z)) + \frac{E\alpha\sigma}{4\kappa} f'(z) \overline{h(z)}. \quad (23)$$

3. Solution for a thermoelectric plate weakened by an elliptic hole

3.1. Boundary conditions. We consider an infinite plane thermoelectric continuum containing an elliptic hole as shown in Figure 1 (left). The major and minor semiaxes of the elliptic hole are denoted by a and b , respectively. The infinite region outside the elliptic hole is referred to as the “matrix”, which is subjected to prescribed remote electric current densities J_x^∞ and J_y^∞ as well as energy flux U_x^∞ and U_y^∞ at the far field. We assume that the boundary of the hole is impervious to both electrons and heat. Thus, the boundary conditions for the electric current and energy flux on the boundary of the hole can be expressed as

$$\int_P^Q J_r ds = 0, \quad (24)$$

$$\int_P^Q U_r ds = 0, \quad (25)$$

where J_r and U_r are the normal electric current density and energy flux, respectively, while P and Q are arbitrary points on the boundary of the hole. Since there is no applied loading on the boundary, both normal and shear stresses are zero, that is,

$$i \int_P^Q (X + iY) ds = 0, \quad (26)$$

where X and Y are the components of surface force on the boundary, respectively [Timoshenko and Goodier 1951].

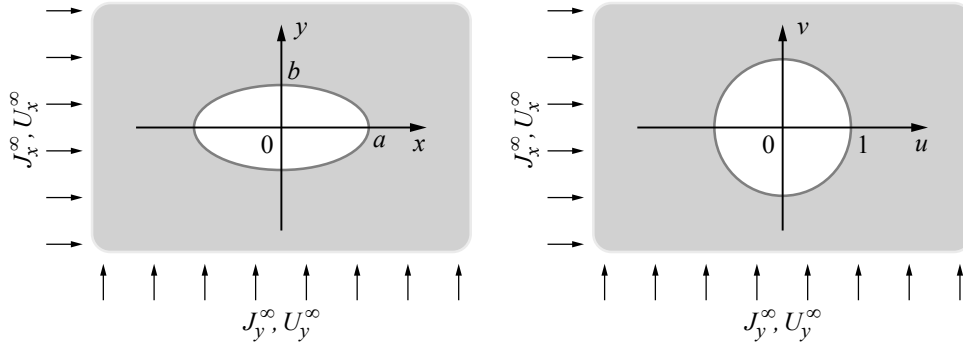


Figure 1. Left: elliptic hole embedded in an infinite thermoelectric plate. Right: the ω -plane after conformal mapping.

Our goal is to determine the temperature and thermal stress distributions around the hole. To this end, consider the conformal mapping

$$z = \omega(w) = R(w + m/w), \quad (27)$$

where $R = \frac{1}{2}(a + b)$, $m = (a - b)/(a + b)$, which maps the interior of the elliptic hole in the z -plane into the unit circle in the ω -plane where $w = u + iv$, as illustrated in Figure 1 (right).

3.2. Electric and thermal fields. Given the prescribed remote electric current density, the complex function $f(z)$ in the matrix can be expressed as

$$f(z) = A_1'z + f_0(z), \quad (28)$$

where $f_0(z)$ is an analytic function, and the coefficient A_1' can be determined by the value of the remote electric current density. The complex function $f(w)$ obtained from (28) via (27) can now be represented in the form

$$f(w) = A_1w + \sum_{k=0}^{\infty} A_{-k}w^{-k}, \quad (29)$$

where $A_1 = -R(J_x^\infty - iJ_y^\infty)/\sigma$. Substituting (7) into the boundary condition (24), we have

$$\int J_r ds = \int J_x dy - J_y dx = \frac{1}{2}\sigma i(f(w) - \overline{f(w)}) = 0. \quad (30)$$

Solving (30) using (29) yields

$$f(w) = A_1w + A_{-1}/w, \quad (31)$$

where $A_{-1} = \bar{A}_1$. Similarly, $g(z)$ can be written as

$$g(z) = B_2'z^2 + B_1'z + g_0(z), \quad (32)$$

and the complex function $g(w)$ in the ω -plane can be represented by

$$g(w) = B_2w^2 + B_1w + \sum_{k=0}^{\infty} B_{-k}w^{-k}, \quad (33)$$

where $B_1 = -R(U_x^\infty - iU_y^\infty)/2\kappa$, $B_2 = -\sigma A_1^2/8\kappa$ according to the energy flux prescribed at infinity. Noting (15), the boundary condition (25) can be rewritten as

$$\int U_r ds = \int U_x dy - U_y dx = \frac{1}{8}\sigma i(f(w)^2 - \overline{f(w)^2}) + i\kappa(g(w) - \overline{g(w)}) = 0. \quad (34)$$

Comparing coefficients of like powers of w^k , $g(w)$ can be determined from (34) as

$$g[w] = B_2 w^2 + B_1 w + \frac{B_{-1}}{w} + \frac{B_{-2}}{w^2}, \quad (35)$$

where $B_{-1} = \bar{B}_1$, $B_{-2} = \bar{B}_2$. This set of equations solves completely the thermal-electric problems of an infinite thermoelectric continuum containing an elliptic hole leading to the complete determination of the field distributions in closed-form. In particular, the temperature and electric potential are determined as

$$T = -\frac{\sigma}{4\kappa}|A_1 w + A_{-1}/w|^2 + 2\operatorname{Re}\left[B_2 w^2 + B_1 w + \frac{B_{-1}}{w} + \frac{B_{-2}}{w^2}\right] + N, \quad (36)$$

$$\phi = \operatorname{Re}[A_1 w + A_{-1}/w] + \frac{\sigma S}{4\kappa}|A_1 w + A_{-1}/w|^2 - 2S\operatorname{Re}\left[B_2 w^2 + B_1 w + \frac{B_{-1}}{w} + \frac{B_{-2}}{w^2}\right] - SN, \quad (37)$$

and the electric current density, thermal flux and energy flux are given by

$$J_x - iJ_y = -\frac{\sigma(A_1 w^2 - A_{-1})}{R(w^2 - m)}, \quad (38)$$

$$Q_x - iQ_y = \frac{\sigma(A_1 w^2 - A_{-1})}{2R(w^2 - m)} \times \left\{ \left(\frac{\sigma S}{2\kappa} \left| A_1 w + \frac{A_{-1}}{w} \right|^2 + \bar{A}_1 \bar{w} + \frac{\bar{A}_{-1}}{\bar{w}} \right) - 4S\operatorname{Re}\left[B_2 w^2 + B_1 w + \frac{B_{-1}}{w} + \frac{B_{-2}}{w^2} \right] - 2SN \right\} - \frac{2\kappa(2B_2 w^4 + B_1 w^3 - B_{-1} w - 2B_{-2})}{Rw(w^2 - m)}, \quad (39)$$

$$U_x - iU_y = -\frac{\sigma(A_1 w^2 - A_{-1})(A_1 w^2 + A_{-1})}{2Rw(w^2 - m)} - \frac{2\kappa(2B_2 w^4 + B_1 w^3 - B_{-1} w - 2B_{-2})}{Rw(w^2 - m)}. \quad (40)$$

3.3. Stress distributions. It is assumed that the matrix is not constrained at infinity and can therefore expand freely there. Integrating $f(z)$ in (31), $h(z)$ is found from (20) to be

$$h(z) = R\left[\frac{1}{2}A_1 w^2 + \frac{mA_{-1}}{2w^2} + (A_{-1} - mA_1)\ln w \right]. \quad (41)$$

Noting the multivalued term appearing in $h(z)$, the functions $\varphi(z)$ and $\psi(z)$ in (22) and (23) can be expressed in the form

$$\varphi(z) = \varphi(w) = \eta_1 \ln w + \varphi_0(w), \quad (42)$$

$$\psi(z) = \psi(w) = \eta_2 \ln w + \psi_0(w). \quad (43)$$

According to (21), the boundary condition in (26) can be rewritten as

$$i \int_P^Q (X + iY) ds = \varphi(z) + z \overline{\varphi'(z)} + \overline{\psi(z)} + \frac{E\alpha\sigma}{8\kappa} h(z) \overline{f(z)} = 0. \quad (44)$$

Substituting (31), (41), (42), and (43) into (44), the unknown functions $\varphi(w)$ and $\psi(w)$ are found to be

$$\varphi[w] = -\frac{E\alpha\sigma R m \bar{A}_1}{16\kappa} \left(\frac{A_1}{w} + \frac{\bar{A}_1}{w^3} \right), \quad (45)$$

$$\begin{aligned} \psi[w] = \frac{E\alpha\sigma R}{8\kappa} (A_1 - m\bar{A}_1) \left(A_1 w + \frac{\bar{A}_1}{w} \right) \ln w - \frac{E\alpha\sigma R \bar{A}_1}{16\kappa} \left(\frac{A_1}{w} + \frac{\bar{A}_1}{w^3} \right) \\ - \frac{E\alpha\sigma m R \bar{A}_1 (1 + mw^2)}{16\kappa (w^2 - m)} \left(\frac{A_1}{w} + \frac{3\bar{A}_1}{w^3} \right). \end{aligned} \quad (46)$$

The stress distributions in (22) and (23) can now be determined completely:

$$\sigma_{11} + \sigma_{22} = \frac{E\alpha\sigma m}{4\kappa} \operatorname{Re} \left[\frac{\bar{A}_1 (A_1 w^2 + 3\bar{A}_1)}{w^2 (w^2 - m)} \right] + \frac{E\alpha\sigma}{4\kappa} \left(A_1 w + \frac{\bar{A}_1}{w} \right) \left(\bar{A}_1 \bar{w} + \frac{A_1}{\bar{w}} \right), \quad (47)$$

$$\begin{aligned} \sigma_{22} - \sigma_{11} + 2i\sigma_{12} \\ = \frac{E\alpha\sigma m \bar{A}_1}{w^2 - m} \left[\frac{A_1 w^4 + 6\bar{A}_1 w^2 - 3m\bar{A}_1}{4\kappa w (w^2 - m)^2} \left(\bar{w} + \frac{m}{\bar{w}} \right) + \frac{A_1 w^2 + 3\bar{A}_1}{8\kappa w^2} \right] \\ + \frac{E\alpha\sigma m \bar{A}_1}{8\kappa} \frac{A_1 (mw^6 + m^2 w^4 + 3w^4 - mw^2) + 3\bar{A}_1 (3mw^4 - m^2 w^2 + 5w^2 - 3m)}{w^2 (w^2 - m)^3} \\ + \frac{E\alpha\sigma}{4\kappa} \frac{A_1 w^2 - \bar{A}_1}{(w^2 - m)} \left[\frac{1}{2} \bar{A}_1 \bar{w}^2 + \frac{mA_1}{2\bar{w}^2} + (A_1 - m\bar{A}_1) \ln \bar{w} \right] \\ + \frac{E\alpha\sigma (A_1 - m\bar{A}_1) [A_1 w^2 + \bar{A}_1 + (A_1 w^2 - \bar{A}_1) \ln w]}{4\kappa (w^2 - m)}. \end{aligned} \quad (48)$$

Noting the expression for A_1 , we see that the thermal stress is completely dependent on the applied electric current in the x and y directions, which makes it possible to suppress the thermal stress by simply adjusting the applied electric current itself.

4. Methods for suppressing thermal stress

4.1. Suppressing thermal stress by adjusting the electric current. In a thermoelectric material, the conversion efficiency H is the main parameter of interest. When the electric current and heat flux flow through a thermoelectric medium, the conversion efficiency can be calculated from the measured physical quantities. Here we select a finite square region of side L containing an elliptic hole (see Figure 2). Without loss of generality, we apply the electric current and energy flux in the y -direction, the conversion efficiency can then be derived as [Harman and Honig 1967]

$$H = \frac{\int_t \phi_2 J_{y2} dx - \int_s \phi_1 J_{y1} dx}{\int_s U_{y1} dx}, \quad (49)$$

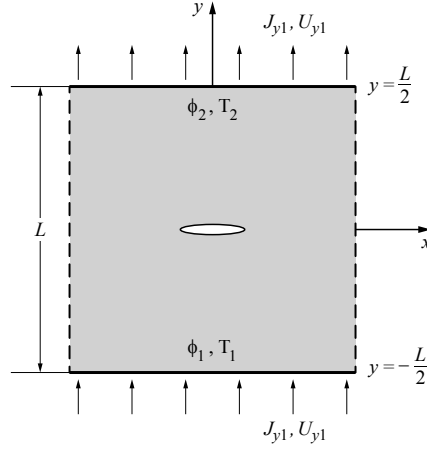


Figure 2. Finite thermoelectric model subjected electric current and energy flux in y -direction.

where s and t denote the entire surface corresponding to $y = -\frac{1}{2}L$ and $y = \frac{1}{2}L$, respectively, while the subscripts 1 and 2 denote the corresponding quantities on s and t , respectively. The conversion efficiency can be optimized with respect to electric current density for given temperatures. For example, if the temperatures on s and t are T_1 and T_2 , respectively, the optimal electric current density for this system is [Yang et al. 2013]

$$J_{\text{opt}} = \frac{\sqrt{2\kappa} \sigma S (T_1 - T_2)}{[\sqrt{2\kappa} + \sqrt{2\kappa \sigma S^2 (T_1 + T_2)}] L}. \quad (50)$$

In other words, the highest conversion efficiency requires the accompaniment of optimal electric current density J_{opt} .

On the other hand, the components of thermal stress in polar coordinates are given by the coordinate transformation formulas [Muskhelishvili 1975]:

$$\sigma_{\rho\rho} + \sigma_{\theta\theta} = \sigma_{11} + \sigma_{22}, \quad (51)$$

$$\sigma_{\theta\theta} - \sigma_{\rho\rho} + 2i\sigma_{\rho\theta} = \frac{w^2 \omega'(w)}{\rho^2 \omega'(w)} (\sigma_{22} - \sigma_{11} + 2i\sigma_{12}), \quad (52)$$

where $\sigma_{\rho\rho}$, $\sigma_{\theta\theta}$, and $\sigma_{\rho\theta}$ are the corresponding normal and shear components in polar coordinates. Since both $\sigma_{\rho\rho}$ and $\sigma_{\rho\theta}$ are zero on the boundary of the elliptic hole, we focus only on the component $\sigma_{\theta\theta}$, which can be derived from (51) and (52) as

$$\sigma_{\theta\theta} = \frac{1}{2} \left[\sigma_{11} + \sigma_{22} + \frac{w^2 \omega'(w)}{\rho^2 \omega'(w)} (\sigma_{22} - \sigma_{11} + 2i\sigma_{12}) \right]. \quad (53)$$

The expanded form of (53) shows that $\sigma_{\theta\theta}$ is a monotonically increasing quadratic function of electric current density. Consequently, both the conversion efficiency and thermal stress depend on the electric current which is therefore confined to a particular range in order to achieve higher conversion efficiency and lower thermal stress.

sample	σ (Sm ⁻¹)	ε (VK ⁻¹)	κ (Wm ⁻¹ K ⁻¹)	E (GPa)	α (K ⁻¹)	μ
Bi ₂ Te ₃	100000	0.00022	1.1	63.00	1.3×10^{-5}	0.23

Table 1. Material parameters of thermoelectric sample [Wu et al. 2014].

4.2. Suppressing thermal stress through vertical electric current. Back to the infinite thermoelectric plate: although the thermal stress can be mitigated by adjusting the electric current, it has a fairly limited role. In order to avoid the influence of electric current on the conversion efficiency, the vertical electric current can be applied to suppress thermal stress around an elliptic hole. For example, consider the case when $\sigma_{\theta\theta}$ has the value

$$\sigma_{\theta\theta} = -\frac{E\alpha m R^2 J_y^{\infty 2}}{2\sigma\kappa(1-m)}, \quad (54)$$

at the point $z = a$ when the material is loaded with a remote electric current in the y -direction. With the additional electric current in the x -direction, $\sigma_{\theta\theta}$ can be shown to be

$$\sigma_{\theta\theta} = \frac{E\alpha R^2 (2J_x^{\infty 2} - mJ_y^{\infty 2})}{2\sigma\kappa(1-m)}. \quad (55)$$

It can be seen that $\sigma_{\theta\theta}$ can be suppressed or totally eliminated by additional electric current at the point $z = a$. More importantly, if the elliptic hole degenerates into a crack, the thermal stress will have a singularity at the crack tip which gives rise to the stress intensity factor corresponding to $\sigma_{\theta\theta}$:

$$K_{\theta\theta} = \lim_{z \rightarrow a} \sqrt{2\pi(z-a)} \sigma_{\theta\theta} = \frac{E\alpha\sqrt{\pi a^5}}{32\sigma\kappa} (2J_x^{\infty 2} - J_y^{\infty 2}). \quad (56)$$

The thermal stress singularity at the crack tip can be eliminated when subjected to the electric current density $J_x^{\infty} = J_y^{\infty}/\sqrt{2}$.

5. Results and discussion

Numerical analyses have been undertaken to further illustrate the effects of electric current on thermal stresses with the material parameters of the corresponding samples listed in Table 1. We first consider the model described in Figure 2. The length of the semimajor axis of the elliptic hole is 0.01 m, while the length and width of the selected sample region are relatively much larger than the size of the elliptic hole. The temperatures on s and t are $T_1 = 800$ K and $T_2 = 300$ K, respectively. Thus, the optimal electric current density can be approximately determined as $J_{\text{opt}} = 1.93 \times 10^5$ A/m², as the elliptic hole has little influence on the conversion optimization efficiency of this system due to its relatively small size.

Under these conditions, the stress component $\sigma_{\theta\theta}$ on the boundary of the elliptic hole is shown in Figure 3 for the difference b , where θ is the angle measured up from the x -axis. It can be seen that the maximum value of positive stress decreases while the maximum negative stress increases as b decreases. Additionally, the stress distribution on the boundary is symmetric around the origin, thereby reducing the amount of computation required in what follows.

Due to the symmetry of the stress field on the boundary, we select two points, $z = a$ and $z = ib$, as samples to analyze the influence of the electric current on the conversion efficiency and corresponding stress

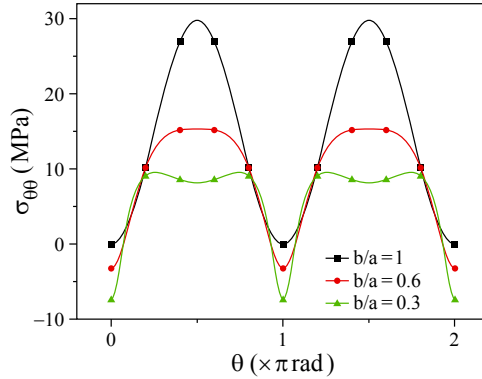


Figure 3. Thermal stress $\sigma_{\theta\theta}$ on the boundary of elliptic hole.

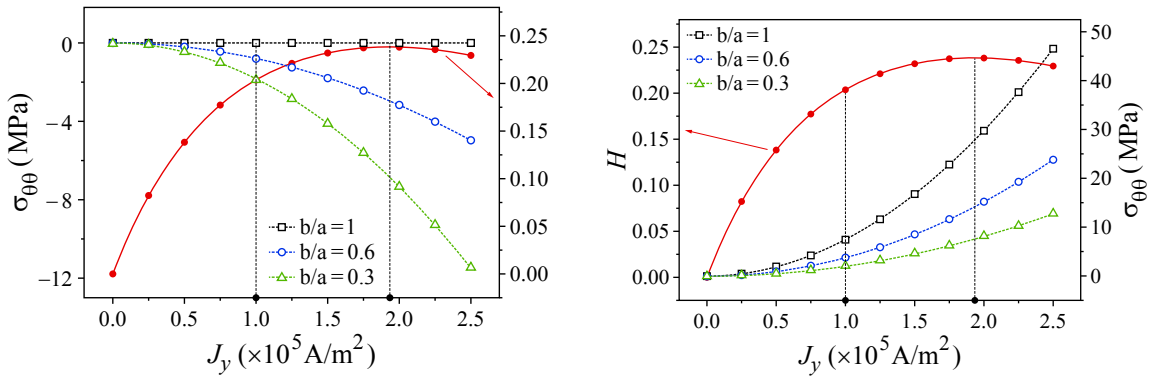


Figure 4. Conversion efficiency versus electric current density: $\sigma_{\theta\theta}$ at the point $z = a$ (left) and $\sigma_{\theta\theta}$ at the point $z = ib$ (right).

distributions. As we can see from Figure 4, the optimal electric current leads to maximum conversion efficiency but also corresponds to higher stresses. Fortunately, the change in the stress distributions is sharper than the conversion efficiency around the optimal electric current. For example, if we decrease the electric current density from J_{opt} to 10^5 A/m², the conversion efficiency will decrease by 14.5%, while all of the stress distributions at the two selected points will decrease by 73.2%. The huge difference between conversion efficiency and thermal stress makes it possible to minimize thermal stress by adjusting the electric current.

Apart from adjusting the electric current in the y -direction, the additional electric current in the x -direction also has the potential to suppress thermal stress. In fact, it has the added advantage of having no effect on the conversion efficiency in the vertical direction and totally neutralizing the thermal stress at a particular point. From Figure 5 we see that the stresses at the point $z = a$ decrease with the increase of J_x^∞ for different values of the semiminor axis of the elliptic hole while maintaining the semimajor axis at $a = 0.01$ m and, in fact, both can be entirely neutralized by electric current.

As noted in Section 4.2, crack tips correspond to singular points of thermal stress in a thermoelectric material but the singularity can be eliminated by additional electric current in the vertical direction. In order to further investigate this phenomenon, we analyze the stress $\sigma_{\theta\theta}$ on the upper boundary of the

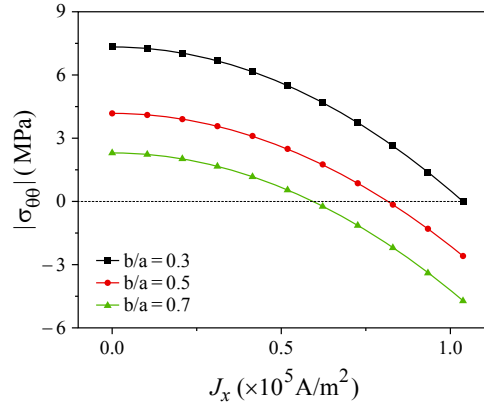


Figure 5. Stress field at the point $z = a$ versus electric current density J_x^∞ .

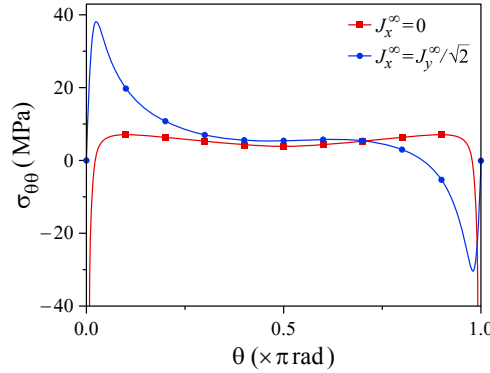


Figure 6. Stress field on the upper boundary of elliptic hole while $b \ll a$.

elliptic hole for the case $b \ll a$ (see Figure 6). The results show that the values of $\sigma_{\theta\theta}$ tend towards negative infinity at the points $z = a$ and $z = -a$ while $J_x^\infty = 0$, and $\sigma_{\theta\theta}$ is totally neutralized by the additional electric current density $J_x^\infty = J_y^\infty/\sqrt{2}$ despite the fact that it also leads to a considerable positive stress.

6. Conclusions

In contrast to traditional heat conduction in common materials, the coupled transport of heat flux and electric current allows for the existence of thermal stress in a simply connected thermoelectric medium which then affects the reliability of thermoelectric devices. Consequently, it becomes important to develop methods for the suppression of thermal stresses in thermoelectric media. In this paper, we have addressed this question in the case of a thermoelectric plate weakened by an elliptic hole. The results show that the thermal stress on the boundary of an elliptic hole can be suppressed by both adjusting the value of the electric current and adding additional vertical electric current. Each method is effective in improving reliability and prolonging the life of thermoelectric devices.

Acknowledgements

Song appreciates the support of the China Scholarship Council. Song and Gao acknowledge the support of the National Natural Science Foundation of China (Grant Nos. 11202099 and 11872203), the Priority Academic Program Development of Jiangsu Higher Education Institutions (PAPD). Schiavone thanks the Natural Sciences and Engineering Research Council of Canada for their support through a Discovery Grant (Grant # RGPIN 155112). The authors would like to thank an anonymous reviewer whose comments have greatly improved the manuscript.

References

- [Callen 1960] H. B. Callen, *Thermodynamics: an introduction to the physical theories of equilibrium thermostatics and irreversible thermodynamics*, Wiley, New York, 1960.
- [Choi et al. 2011] H.-S. Choi, W.-S. Seo, and D.-K. Choi, "Prediction of reliability on thermoelectric module through accelerated life test and Physics-of-failure", *Electron. Mater. Lett.* **7** (2011), 271.
- [Göktun 36] S. Göktun, "Design considerations for a thermoelectric refrigerator", *Energy Convers. Manage.* **36**:12 (36), 1197–1200.
- [Harman and Honig 1967] T. C. Harman and J. M. Honig, *Thermoelectric and thermomagnetic effects and applications*, McGraw Hill, New York, 1967.
- [Kim and Chun 2007] T.-S. Kim and B.-S. Chun, "Microstructure and thermoelectric properties of n- and p-type Bi₂Te₃ alloys by rapid solidification processes", *J. Alloys Compd.* **437**:1-2 (2007), 225–230.
- [Kim et al. 2006] W. Kim, J. Zide, A. Gossard, D. Klenov, S. Stemmer, A. Shakouri, and A. Majumdar, "Thermal conductivity reduction and thermoelectric figure of merit increase by embedding nanoparticles in crystalline semiconductors", *Phys. Rev. Lett.* **96**:4 (2006), 045901.
- [Liu 2012] L. Liu, "A continuum theory of thermoelectric bodies and effective properties of thermoelectric composites", *Int. J. Eng. Sci.* **55** (2012), 35–53.
- [Milton 2002] G. W. Milton, *The theory of composites*, Cambridge University Press, 2002.
- [Muskhelishvili 1975] N. I. Muskhelishvili, *Some basic problems of mathematical theory of elasticity*, Noordhoff, Leyden, 1975.
- [Okamura et al. 2010] C. Okamura, T. Ueda, and K. Hasezaki, "Preparation of single-phase ZnSb thermoelectric materials using a mechanical grinding process", *Mater. Trans.* **51**:5 (2010), 860–862.
- [Omer and Infield 1998] S. A. Omer and D. G. Infield, "Design optimization of thermoelectric devices for solar power generation", *Sol. Energy Mater. Sol. Cells* **53**:1 (1998), 67–82.
- [Parkus 1968] H. Parkus, *Thermoelasticity*, Blaisdell Pub. Co., Waltham, MA, 1968.
- [Pei et al. 2011] Y. Pei, A. LaLonde, S. Iwanaga, and G. J. Snyder, "High thermoelectric figure of merit in heavy hole dominated PbTe", *Energy Environ. Sci.* **4**:6 (2011), 2085–2089.
- [Riffat and Ma 2003] S. B. Riffat and X. Ma, "Thermoelectrics: a review of present and potential applications", *Appl. Therm. Eng.* **23**:8 (2003), 913–935.
- [Song et al. 2015] H.-P. Song, C.-F. Gao, and J. Li, "Two-dimensional problem of a crack in thermoelectric materials", *J. Therm. Stress* **38**:3 (2015), 325–337.
- [Song et al. 2017] K. Song, H. P. Song, and C. F. Gao, "Macro-performance of multilayered thermoelectric medium", *Chinese Phys. B* **26** (2017), 127307.
- [Timoshenko and Goodier 1951] S. P. Timoshenko and J. N. Goodier, *Theory of elasticity*, McGraw Hill, New York, 1951.
- [Tritt and Subramanian 2006] T. M. Tritt and M. A. Subramanian, "Thermoelectric materials, phenomena, and applications: a bird's eye view", *MRS Bulletin* **31**:3 (2006), 188–198.
- [Wu et al. 2014] Y. Wu, T. Ming, X. Li, T. Pan, K. Peng, and X. Luo, "Numerical simulations on the temperature gradient and thermal stress of a thermoelectric power generator", *Energy Convers. Manage.* **88** (2014), 915–927.

- [Xuan 2002] X. C. Xuan, "Optimum design of a thermoelectric device", *Semicond. Sci. Technol.* **17**:2 (2002), 114.
- [Yang et al. 2012] Y. Yang, S. H. Xie, F. Y. Ma, and J. Y. Li, "On the effective thermoelectric properties of layered heterogeneous medium", *J. Appl. Phys.* **111** (2012), 013510.
- [Yang et al. 2013] Y. Yang, F. Y. Ma, C. H. Lei, Y. Y. Liu, and J. Y. Li, "Is thermoelectric conversion efficiency of a composite bounded by its constituents?", *Appl. Phys. Lett.* **102**:5 (2013), 053905.
- [Yu et al. 2012] R. Yu, P. Zhai, G. Li, and L. Liu, "Molecular dynamics simulation of the mechanical properties of single-crystal bulk Mg_2Si ", *J. Electron. Mater.* **41**:6 (2012), 1465–1469.
- [Zhao and Tan 2014] D. Zhao and G. Tan, "A review of thermoelectric cooling: materials, modeling and applications", *Appl. Therm. Eng.* **66**:1-2 (2014), 15–24.

Received 3 Dec 2018. Revised 10 Dec 2018. Accepted 16 Dec 2018.

KUN SONG: ksong3@ualberta.ca

Institute of Aerospace, Nanjing University of Aeronautics and Astronautics, Nanjing, China

HAO-PENG SONG: hpsong@nuaa.edu.cn

Department of Software Engineering, Nanjing University of Aeronautics and Astronautics, Nanjing, China

PETER SCHIAVONE: pschiavo@ualberta.ca

Department of Mechanical Engineering, University of Alberta, Edmonton, AB, Canada

CUN-FA GAO: cfgao@nuaa.edu.cn

State Key Laboratory of Mechanics and Control of Mechanical Structures, Nanjing University of Aeronautics and Astronautics, Nanjing, China

JOURNAL OF MECHANICS OF MATERIALS AND STRUCTURES

msp.org/jomms

Founded by Charles R. Steele and Marie-Louise Steele

EDITORIAL BOARD

ADAIR R. AGUIAR	University of São Paulo at São Carlos, Brazil
KATIA BERTOLDI	Harvard University, USA
DAVIDE BIGONI	University of Trento, Italy
MAENGHYO CHO	Seoul National University, Korea
HUILING DUAN	Beijing University
YIBIN FU	Keele University, UK
IWONA JASLUK	University of Illinois at Urbana-Champaign, USA
DENNIS KOCHMANN	ETH Zurich
MITSUTOSHI KURODA	Yamagata University, Japan
CHEE W. LIM	City University of Hong Kong
ZISHUN LIU	Xi'an Jiaotong University, China
THOMAS J. PENCE	Michigan State University, USA
GIANNI ROYER-CARFAGNI	Università degli studi di Parma, Italy
DAVID STEIGMANN	University of California at Berkeley, USA
PAUL STEINMANN	Friedrich-Alexander-Universität Erlangen-Nürnberg, Germany
KENJIRO TERADA	Tohoku University, Japan

ADVISORY BOARD

J. P. CARTER	University of Sydney, Australia
D. H. HODGES	Georgia Institute of Technology, USA
J. HUTCHINSON	Harvard University, USA
D. PAMPLONA	Universidade Católica do Rio de Janeiro, Brazil
M. B. RUBIN	Technion, Haifa, Israel

PRODUCTION production@msp.org

SILVIO LEVY Scientific Editor

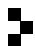
Cover photo: Ev Shafir

See msp.org/jomms for submission guidelines.

JoMMS (ISSN 1559-3959) at Mathematical Sciences Publishers, 798 Evans Hall #6840, c/o University of California, Berkeley, CA 94720-3840, is published in 10 issues a year. The subscription price for 2019 is US \$635/year for the electronic version, and \$795/year (+\$60, if shipping outside the US) for print and electronic. Subscriptions, requests for back issues, and changes of address should be sent to MSP.

JoMMS peer-review and production is managed by EditFLOW[®] from Mathematical Sciences Publishers.

PUBLISHED BY

 **mathematical sciences publishers**
nonprofit scientific publishing

<http://msp.org/>

© 2019 Mathematical Sciences Publishers

Journal of Mechanics of Materials and Structures

Volume 14, No. 1

January 2019

The role of rheology in modelling elastic waves with gas bubbles in granular fluid-saturated media	ADHAM A. ALI and DMITRY V. STRUNIN	1
Some general theorems for local gradient theory of electrothermoelastic dielectrics	OLHA HRYTSYNA and HALYNA MOROZ	25
Effect of surface elasticity on stress intensity factors near mode-III crack tips	XIAN-FANG LI	43
Analytical investigation of free vibrations of a bounded nonlinear bulk-elastic medium in a field of mass forces	EUGENE I. RYZHAK and SVETLANA V. SINYUKHINA	61
A modified shear-lag model for prediction of stress distribution in unidirectional fibrous composites considering interphase	MOHAMMAD HASSAN ZARE and MEHDI MONDALI	97
Nonlinear free vibration of nanobeams based on nonlocal strain gradient theory with the consideration of thickness-dependent size effect	WEI CHEN, LIN WANG and HU-LIANG DAI	119
Energy-maximizing holes in an elastic plate under remote loading	SHMUEL VIGDERGAUZ and ISAAC ELISHAKOFF	139
Anisotropic multimaterial lattices as thermal adapters	MARINA M. TOROPOVA	155
Thermal stress around an elliptic hole weakened by electric current in an infinite thermoelectric plate	KUN SONG, HAO-PENG SONG, PETER SCHIAVONE and CUN-FA GAO	179



1559-3959(2019)14:1;1-X